



## Molecular Crystals and Liquid Crystals

Publication details, including instructions for authors and subscription information:

<http://www.tandfonline.com/loi/gmcl20>

### B 2 -B 4 DIMORPHISM IN A NEW SERIES OF BANANA-SHAPED MESOGENS

H. Nádasi<sup>a</sup>, Ch. Lischka<sup>a</sup>, W. Weissflog<sup>a</sup>, I. Wirth<sup>a</sup>, S. Diele<sup>a</sup>, G. Pelzl<sup>a</sup> & H. Kresse<sup>a</sup>

<sup>a</sup> Institut für Physikalische Chemie, Mühlpforte 1, Martin-Luther-Universität Halle-Wittenberg, Halle, D-06108

Version of record first published: 18 Oct 2010

To cite this article: H. Nádasi, Ch. Lischka, W. Weissflog, I. Wirth, S. Diele, G. Pelzl & H. Kresse (2003): B 2 -B 4 DIMORPHISM IN A NEW SERIES OF BANANA-SHAPED MESOGENS, *Molecular Crystals and Liquid Crystals*, 399:1, 69-84

To link to this article: <http://dx.doi.org/10.1080/15421400390225471>

PLEASE SCROLL DOWN FOR ARTICLE

Full terms and conditions of use: <http://www.tandfonline.com/page/terms-and-conditions>

This article may be used for research, teaching, and private study purposes. Any substantial or systematic reproduction, redistribution, reselling, loan, sub-licensing, systematic supply, or distribution in any form to anyone is expressly forbidden.

The publisher does not give any warranty express or implied or make any representation that the contents will be complete or accurate or up to date. The accuracy of any instructions, formulae, and drug doses should be independently verified with primary sources. The publisher shall not be liable

for any loss, actions, claims, proceedings, demand, or costs or damages whatsoever or howsoever caused arising directly or indirectly in connection with or arising out of the use of this material.

## **B<sub>2</sub>-B<sub>4</sub> DIMORPHISM IN A NEW SERIES OF BANANA-SHAPED MESOGENS**

*H. Nádasi, Ch. Lischka, W. Weissflog,\* I. Wirth, S. Diele,  
G. Pelzl, and H. Kresse*

*Martin-Luther-Universität Halle-Wittenberg, Institut für  
Physikalische Chemie, Mühlpforte 1, D-06108 Halle*

*A new series of five-ring banana-shaped mesogens derived from isophthalaldehyde was synthesized and investigated. Some of the compounds exhibit a B<sub>2</sub>-B<sub>4</sub> dimorphism. The mesophases were characterized alternatively by optical methods, X-ray studies, and dielectric and electro-optical measurements.*

**Keywords:** liquid crystals; banana-shaped mesogens; dielectric measurements; X-ray diffraction; electro-optical studies

### **INTRODUCTION**

In 1996 Niori et al. reported new mesophases formed by bent-shaped molecules [1]. Since ferroelectricity was observed in several phases of such nonchiral compounds, these mesogens have turned into one of the most interesting subfields of liquid crystals. Although a number of new materials with bent molecular shape were synthesized in the past few years [2–6], the knowledge about structure-property relationships is relatively limited in comparison to calamitic liquid crystals. Up to now, so-called B phases were found for banana-shaped molecules consisting of five, six, or seven aromatic rings, having a bending angle of about 105–140° between the two half-parts. In addition, it is known that the groups connecting the aromatic rings have a strong influence. Thus, looking at banana-shaped mesogens, that consist of five benzene rings which are connected by two carboxylic and two azomethine linking groups, the variation of the positions and the direction of these groups leads to very different mesophase behavior. Some

(Received 16 November 2000; in final form 4 September 2001)

The authors thank the “Deutsche Forschungsgemeinschaft” and the “Fond der Chemischen Industrie” for the support of this work.

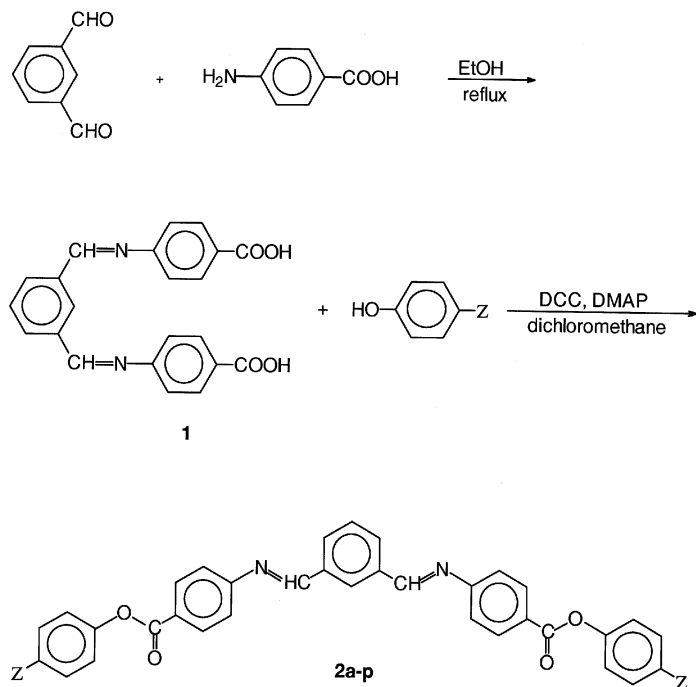
\*Corresponding author. E-mail: weissflog@chemie.uni-halle.de

derivatives exhibit mesophase stability up to 180°C; for other isomers no liquid crystalline state could be detected [2].

We synthesized a new series of banana-shaped compounds in which only the arrangement of the connecting groups is different in comparison with isomeric compounds reported by Sekine et al. [7] and Bedel et al. [8]. Furthermore, not only was the length of the aliphatic chains varied but also the electronic properties of the terminal groups. Moreover, we examined the reaction pathway to be suitable for the synthesis of deuterium-labeled derivatives. We are preparing such deuterated compounds to obtain more information with NMR about the real molecular conformation, which is of importance for understanding the phase structures of banana-shaped mesogens [9,10].

## MATERIALS

The new symmetrically substituted banana-shaped compounds **2** were synthesized according to the reaction pathway shown in Scheme 1. After



**SCHEME 1**

condensation of isophthalaldehyde with 4-aminobenzoic acid the resulting dicarboxylic acid **1** was esterified with several 4-substituted phenols to give the final products **2** (Scheme 1).

### 1,3-phenylene bis(methyliminobenzoic Acid) **1**

5.0 g (0.037 mol) isophthalaldehyde and 10.13 g (0.074 mol) 4-aminobenzoic acid were dissolved in boiling ethanol and heated under reflux for 4 h. After cooling the precipitate was separated and digested by hot ethanol. Substance **1** was recrystallized from DMF/toluene. Yield: 9.20 g (67 %). m.p. > 300°C (decomp.).

### Isophthalaldene bis(4-(4-subst.-phenyloxycarbonyl)aniline) **2**

First 3.72 g (0.1 mmol) of the dicarboxylic acid **1** and 0.22 mmol of the related 4-substituted phenol was reacted in dichloromethane in the presence of DCC (0.26 mmol) and DMAP as catalyst. The mixture was stirred at room temperature for about one week. After filtration the dicyclohexylurea the dichloromethane was evaporated. Residue of the urea can be removed by extraction the raw material with hot ethanol. The crude product was recrystallized more than three times from toluene.

Yields: about 30–40%.

The analytical data are given for **2d**: <sup>1</sup>H NMR (400 MHz, CDCl<sub>3</sub>) δ (ppm): 8.5 (2H, s, CH=N), 8.4 (1H, s, ArH), 8.22–8.24 (4H, d, Ar-H), 8.07–8.09 (2H, s, Ar-H), 7.65 (1H t, Ar-H) 7.09–7.64 (8H, m, Ar-H), 6.89–6.93 (4H, m, Ar-H), 3.93–3.96 (4H, t, OCH<sub>2</sub>), 1.73–1.80 (4H, t, OCH<sub>2</sub>CH<sub>2</sub>), 1.23–1.49 (20H, m, CH<sub>2</sub>), 0.86–0.89 (6H, m, CH<sub>3</sub>)

For all compounds **2a–2p** the melting and phase transition temperatures as well as the transition enthalpies are listed in Table 1.

## EXPERIMENTAL

The temperatures and enthalpies of the phase transitions were determined by differential scanning calorimetry (DSC 7, Perkin-Elmer) at a heating rate of 5 Kmin<sup>-1</sup>. The microscopic textures were analyzed using a polarizing microscope (Leitz Orthoplan) equipped with a heating-stage (Linkam 700THM 600/S). X-ray investigations on non-oriented samples were carried out using the Guinier method (Huber Diffraktionstechnik GmbH) and—for some supplementary measurements—a small angle camera equipped with a position sensitive detector was used. In all X-ray experiments the temperature was controlled to be better than ±1 K.

**TABLE 1** The transition temperatures (C°) and transition enthalpies (kJ/mol) of compounds **2a-p**

Compound	Z	Cr	B <sub>4</sub>		B <sub>2</sub>		I
2a	OC <sub>6</sub> H <sub>11</sub>	•	156 53.01	–	–		•
2b	OC <sub>6</sub> H <sub>13</sub>	•	156 54.4	–	–		•
2c	OC <sub>7</sub> H <sub>15</sub>	•	132 33.3	•	154 53.5	(• 146) 14.5	•
2d	OC <sub>8</sub> H <sub>17</sub>	•	126 31.7	•	148 13.4	• 152 54.1	•
2e	OC <sub>9</sub> H <sub>19</sub>	•	132 45.8	•	145 37.2	• 149 12.0	•
2f	OC <sub>10</sub> H <sub>21</sub>	•	131 43.5	•	148 39.4	• 153 15.8	•
2g	OC <sub>12</sub> H <sub>25</sub>	•	136 53.5	•	145 38.1	• 154 15.4	•
2h	C <sub>8</sub> H <sub>17</sub>	•	127 31.8	–		(• 114)*	•
2i	C <sub>12</sub> H <sub>25</sub>	•	123 35.1	–		(• 121) 12.6	•
2j	COC <sub>6</sub> H <sub>13</sub>	•	176 89.9				•
2k	COC <sub>7</sub> H <sub>15</sub>	•	173 74.7	–	–		•
2l	COC <sub>9</sub> H <sub>19</sub>	•	167 70.6	–	–	–	•
2m	CN	•	243 51.8	–	–		•
2n	C <sub>2</sub> H <sub>4</sub> CN	•	189 61.2	–	–		•
2o	COOC <sub>6</sub> H <sub>13</sub>	•	158 66.5	–	–		•
2p	COOC <sub>10</sub> H <sub>21</sub>	•	151 78.3	–	–		•

\*This transition could not be measured with DSC.

Electro-optical investigations were made using the usual experimental setup where the cells were heated on the hot-stage of the polarizing microscope and the voltage signals were generated by a power supply (8116 A, Hewlett-Packard). Dielectric studies were carried out on non-oriented samples in a brass capacitor coated with gold. The cell ( $d = 0.05$  mm) was calibrated with cyclohexane. Capacity and resistance were measured in the frequency range from 0.1 Hz to 10 MHz using the Solartron Schlumberger Impedance Analyzer Si 1260 and a Chelsea Interface.

## EXPERIMENTAL RESULTS

### Optical Investigations and X-ray Studies

As can be seen from Table 1, liquid crystalline properties were found for the alkoxy- and alkyl-substituted derivatives **2c–2i** only by polarization-microscopic investigations. It should be mentioned that both types of terminal groups have electron-donating properties. In the case of terminal alkanoyl or alkyloxycarbonyl groups, which have a negative mesomeric effect, no mesophases could be detected. One reason could be that the melting points are relatively high. However, the derivative **2p**, for example, could be supercooled up to 110°C, but no mesophase could be observed. This could be a hint that the electronic properties of the terminal substituents are more important than is thought to be for calamitic mesogens.

Because both alkyl-substituted homologues **2h** and **2i** exhibit a metastable B<sub>2</sub> phase only, all furthergoing investigations were done with alkoxy-substituted compounds.

In Figure 1 the transition temperatures of the alkoxy-substituted homologues **2a–2g** are drawn versus the chain length. Starting with the heptyloxy derivative **2c**, all alkoxy compounds exhibit the dimorphism B<sub>2</sub>-B<sub>4</sub>. The longer the terminal chains are, the broader the existence range of the B<sub>2</sub> phase is.

At the first heating the transition Cr-B<sub>4</sub> shows up by the nearly complete disappearance of the birefringence of the initial crystals; meanwhile, the crystal habitus remains unchanged. The B<sub>2</sub> phase, which exhibits a grainy

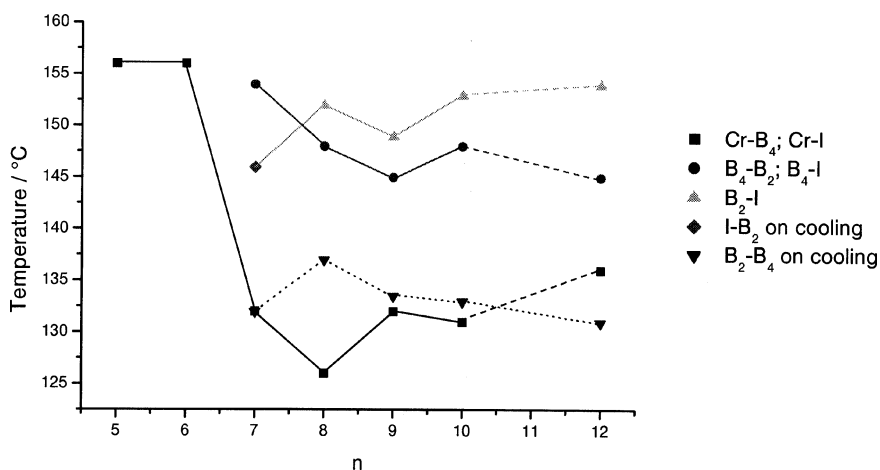


**FIGURE 1** The transition temperatures of the alkoxy-substituted compounds **2a–2g**.

fan-shaped texture, possesses relatively low viscosity. On cooling, the transition  $B_2$ - $B_4$  shows a strong hysteresis. As shown in Figure 1, in most cases the  $B_2$  phase can be supercooled by about 10–15 K. With decreasing temperature, the  $B_4$  phase appears with a blue “color” consistently with the description in literature [7, 11–14]. In some samples the  $B_4$  phase grows from the  $B_2$  phase in typical pattern reminiscent of annual rings of trees, see Figure 2. The transition of the  $B_4$  phase in the crystalline state is considerably delayed, and a slow crystallization can be observed at room temperature after several weeks or by annealing the sample at about 100°C for some hours.

The assignment of the  $B_2$  and  $B_4$  phases has been supported by the results of X-ray diffraction experiments. In the initial solid state a number of sharp reflections in the small- and wide-angle region have been recorded. At the transition into the  $B_4$  phase the wide-angle reflections have been strongly broadened, which is clearly seen in comparison with the pattern of the crystalline state, see Figure 3a. This behavior is reported to be specific for the  $B_4$  phase [2,10]. The maxima of the main scattering are observed at nearly the same scattering angles as the main reflections of the crystalline phase. This broadening of the reflection in the  $B_4$  phase can be explained by a strong decrease of the domain size at the transition into the  $B_4$  phase.

The wide-angle region in the  $B_2$  phase (see Figure 3b) displays only a broad diffuse scattering (around  $\theta \sim 10^\circ$ ) and gives evidence for a liquid-like order in the smectic layers. The layer structure is indicated by two Bragg reflections in the small-angle region (first and second order). The layer spacing  $d$  was found to be clearly lower than the molecule length  $L$  for a bent-shaped conformation (assuming a bending angle of  $120^\circ$ ); e.g., for compound **2e** the  $d$ -value is 4.1 nm, whereas  $L$  is 5 nm. This result points to a tilt of the molecules and is compatible with a  $B_2$  phase.

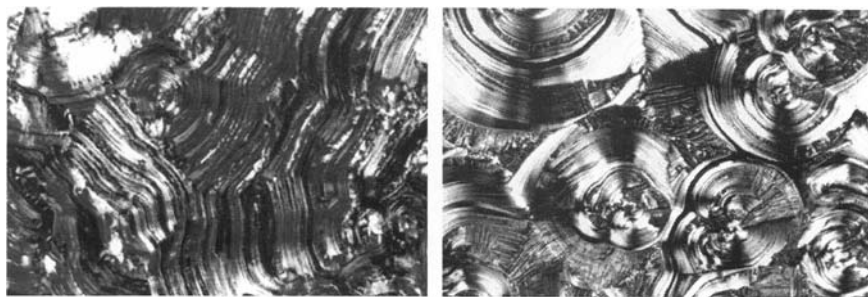
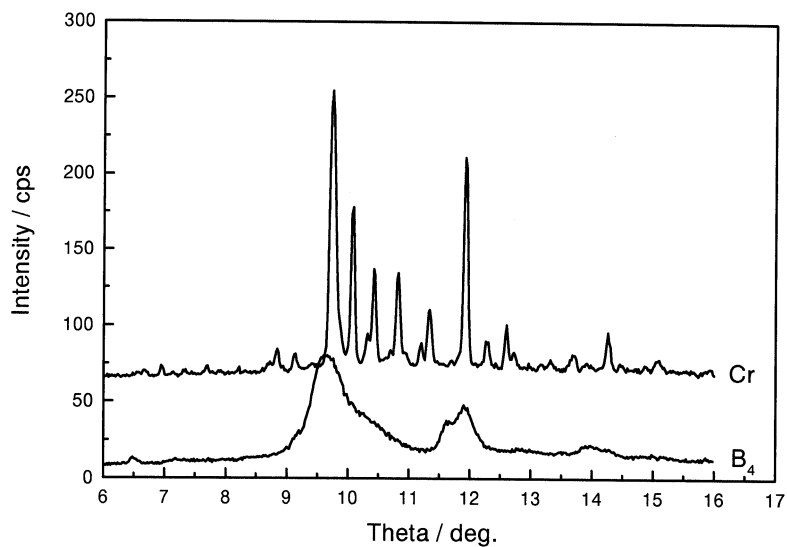
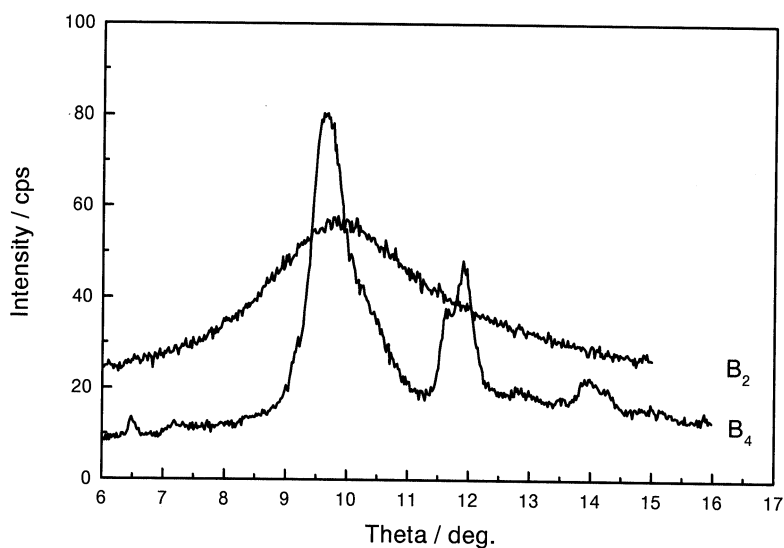


**FIGURE 2** The characteristic feature of the  $B_4$  phase is the blue reflection color (left). In addition, there are some regions with stronger birefringent concentric domains (right).





a)



b)

**FIGURE 3** Comparison of the wide-angle scattering of compound **2e** (a) in the B<sub>4</sub> and crystalline phase and (b) in the B<sub>2</sub> and B<sub>4</sub> phases. The diagram were taken with a Guinier Goniometer.

## Electro-optical Behavior

On cooling the isotropic liquid the B<sub>2</sub> phase preferably forms batonnets with irregular stripes perpendicular to the long axis. On applying an electric field a SmA-like fan-shaped texture arises above the threshold. Depending on the surface conditions and on the history of the sample racemic or homochiral ground states were observed. In the first case the fan-shaped texture of the switched state was independent of the polarity of the field. In homochiral regions the switched state was different for different signs of the applied electric field. Such behavior is illustrated in Figure 4. On the other hand, on applying a triangular voltage of a sufficiently high amplitude, two current peaks were recorded per half period, indicating an antiferroelectric ground state (see Figure 5). The spontaneous polarization could be estimated to be 150 nCcm<sup>-2</sup>.

## Dielectric Behavior

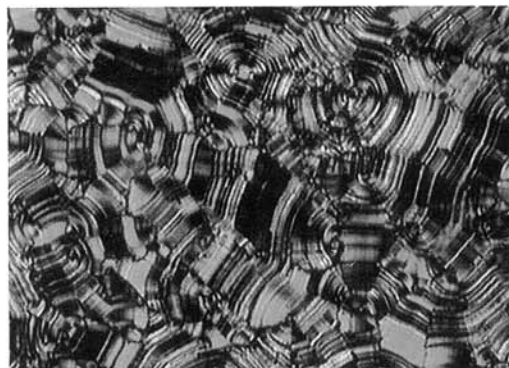
Dielectric studies were carried out on the compound **2e** in the frequency range from 0.1 Hz to 10 MHz. The sample could not be oriented by a magnetic field. Dielectric absorption ( $\varepsilon'$ ) and dispersion ( $\varepsilon''$ ) curves obtained from the first cooling run are shown in the Figure 6. In Figure 7 only the dispersion data of the B<sub>4</sub> phase measured on heating are given.

The experimental data were fitted to the real and imaginary part of Equation (1) to extract the specific behavior of the different phases. The equation consists of two COLE-COLE mechanisms (terms 2 and 3), a conductivity contribution (term 4) and term 5 for the description of the capacitance of the double layer at low frequencies:

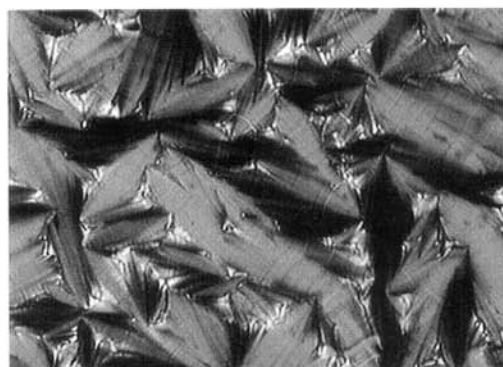
$$\varepsilon^* = \varepsilon_2 + \frac{\varepsilon_0 - \varepsilon_1}{1 + (j\omega\tau_1)^{1-\alpha_1}} + \frac{\varepsilon_1 - \varepsilon_2}{1 + (j\omega\tau_2)^{1-\alpha_2}} + \frac{jA}{f} + \frac{B}{f^N}, \quad (1)$$

with  $\varepsilon_i$  low and high frequency limits of the dielectric permittivity,  $\omega = 2\pi f$  ( $f$  is frequency),  $\tau_i$  is relaxation times,  $\alpha$  is Cole-Cole distribution parameters, and the conductivity term  $A$  (specific conductivity  $\sigma = A \cdot 2 \cdot \pi \cdot \varepsilon^0$ ,  $\varepsilon^0 = 8.85 \cdot 10^{-12}$  As/Vm) as well as  $B$  and  $N$  as further fit parameters describing the capacity of the double layer. For the low frequency mechanism in one phase, generally the limits of the dielectric permittivity  $\varepsilon_0$  and  $\varepsilon_1$  are used.

The obtained limits of the dielectric permittivity are presented in Figure 8. Within the experimental error dielectric absorption in the isotropic phase was not found. The measured dielectric permittivity in the isotropic phase  $\varepsilon_0(I)$  of about 4 indicates that there must be an additional dielectric absorption range in the GHz-region associated with the reorientation of the dipoles about the long axis of the molecules. As usual, the dielectric permittivities  $\varepsilon_0$  and  $\varepsilon_1$  strongly increase at the transition into the B<sub>2</sub> phase



a)



b)



c)

**FIGURE 4** The optical textures (compound **2e**, 6  $\mu\text{m}$  thick EHC cell, 142°C, (a) – 44V, (b) = 0V, c) +44V) are different for an opposite sign of the applied field, that means the dark regions of Figure 4a correspond to bright ones in Figure 4c and vice versa.

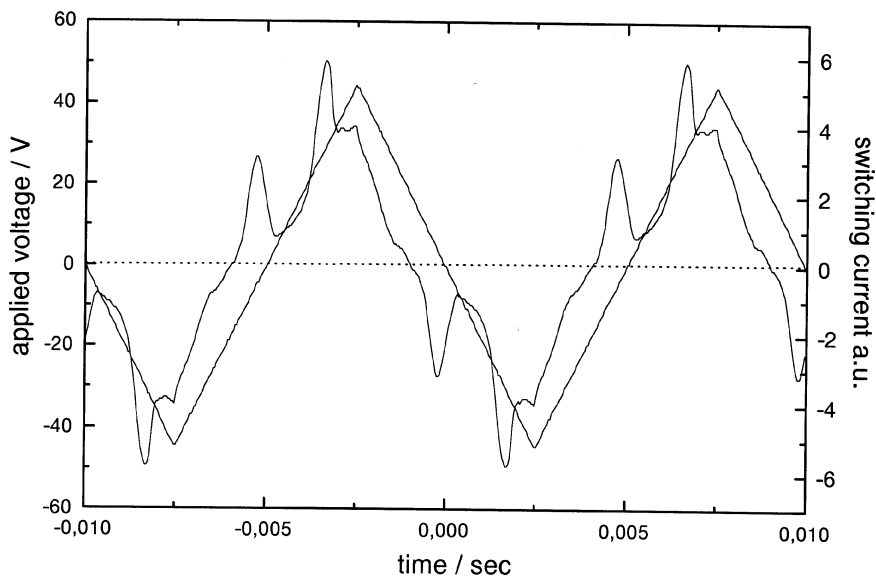


**FIGURE 5** Switching current response in the  $B_2$  phase of compound **2e** obtained by applying a triangular voltage (5  $\mu\text{m}$  thick EHC cell, 140°C,  $\pm 45$  V, 100 Hz).

pointing to a low frequency absorption connected with a ferroelectric superstructure [15–17] and the formation of a ferroelectric short range order of the perpendicular dipole moments.

A clear evidence for a low frequency absorption in the  $B_4$  phase is given in Figure 8. The existence of this absorption range was supposed in a former investigation, but it could not be clearly differentiated from the increasing dielectric permittivity due to the double layer [18]. The high frequency limit of this relaxation process seems to be too high to accept that there is no additional dynamics at high frequencies in the  $B_4$  phase. On the other hand, we could not observe a decrease of the  $\varepsilon$ -values within 14 days, which may be related to a transition into the solid phase. Thus, the question of whether there exists a classical solid phase without any relaxation and a smaller dielectric permittivity at low temperatures cannot be answered in this case. At temperatures below 130°C the low frequency absorption could not be separated from the increase of the dielectric permittivities due to the double layer. Figure 9 shows the dielectric relaxation times. A mean activation energy of the high frequency relaxation ( $\tau_2$ ) of  $220 \pm 50$  kJmol<sup>-1</sup> was calculated for the small temperature range of the  $B_2$  state.

Astonishingly, the relaxation times of the low frequency mechanism in the  $B_2$  phase and that of the  $B_4$  phase are in one line. A common activation

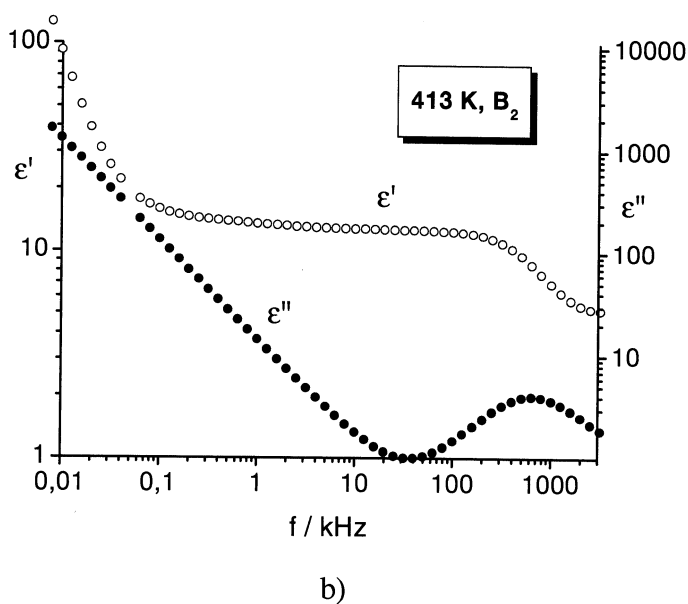
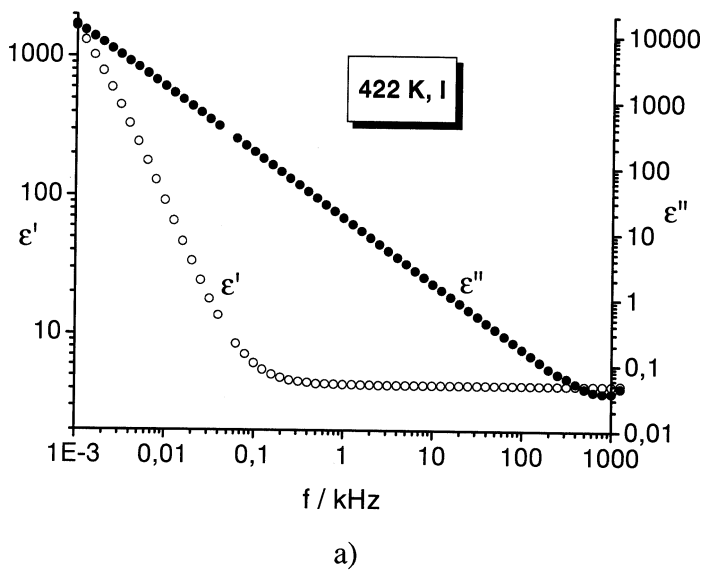


**FIGURE 6** Dielectric permittivity ( $\epsilon'$ ) and losses ( $\epsilon''$ ) of compound **2e** in the isotropic (a) and B<sub>2</sub> phase (b).

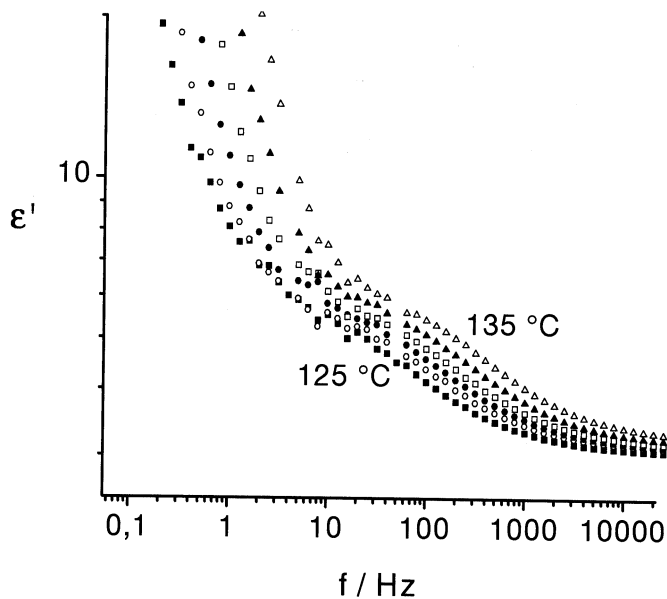


**FIGURE 7** Dispersion data of compound **2e** in the  $B_4$  phase measured on heating.

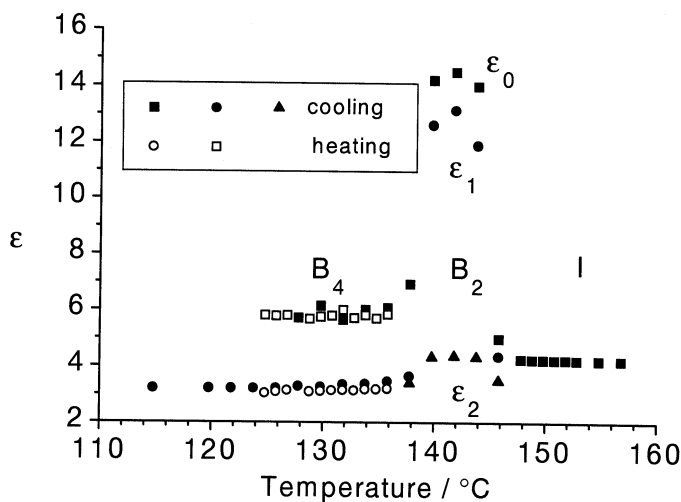
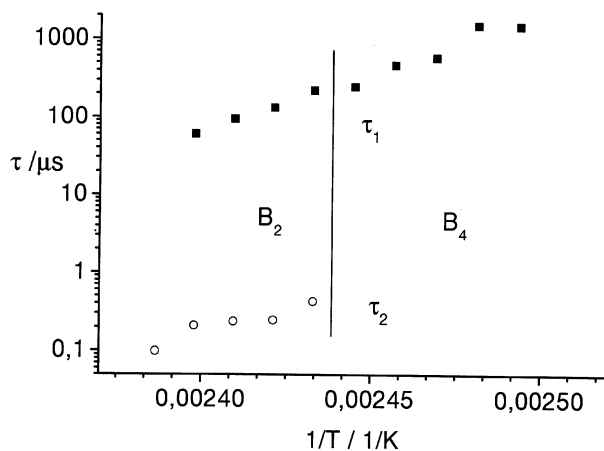
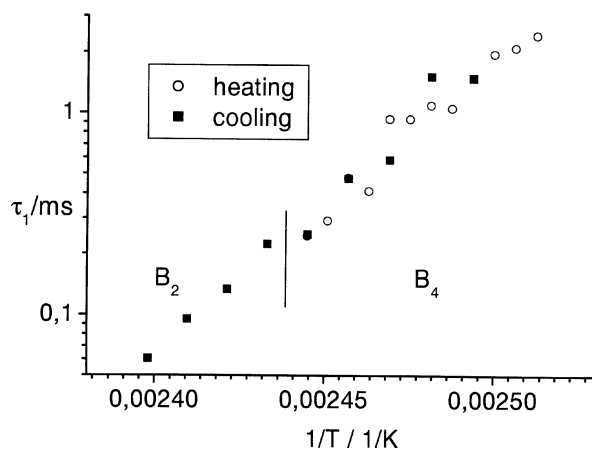


**FIGURE 8** The limits of the dielectric permittivities according to Equation (1) in different phases for cooling and heating.



a)



b)

**FIGURE 9** (a) The relaxation times  $\tau_1$  and  $\tau_2$  in the  $B_2$  and  $B_4$  phase of compound **2e** on cooling; (b) The relaxation times  $\tau_1$  of the low frequency process obtained from measurements on cooling and heating.

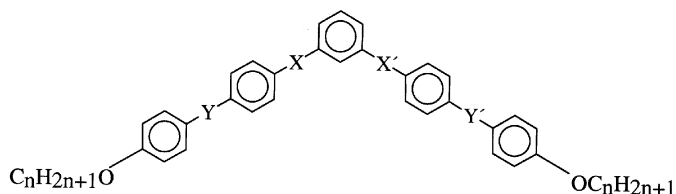
energy for both phases of  $(275 \pm 20)$  kJ was calculated. The dielectric increments ( $\Delta = \epsilon_0 - \epsilon_1$ ) of the relaxation in the  $B_4$  phase are constant within the experimental error (see Figure 8). There is no critical behavior

near to the transition into the  $B_2$  phase at about 139°C. Using this hypothesis one has to explain why the dynamics for the reorientation about the long molecular axis cannot be observed in the  $B_4$  state. It seems to be unbelievable that a collective mechanism in the same liquid crystal is faster than a molecular motion. The obvious explanation is that we observe in the  $B_4$  phase the reorientation about the long molecular axes and no collective motion. The agreement between the relaxation process in the  $B_4$  phase and the low frequency process in the  $B_2$  phase is by chance. To prove this further measurements on different samples are necessary. Another possibility is a Maxwell-Wagner-relaxation at interfaces between small solid particles. In this case we have to explain why this relaxation in the  $B_2$  phase appears, but not in the  $B_4$  phase. Anyway, there is an additional relaxation range which is not compatible with a classical solid modification.

## DISCUSSION

As summarized in Table 2, three isomeric series of five-ring bent mesogens having the chains length  $n = 5-10, 12$  are known up to now. With the resorcinol esters, reported by Sekine et al. in 1997 [7], basic investigations were performed in the field of banana-shaped liquid crystals.  $B_1$ ,  $B_2$ ,  $B_3$ , and  $B_4$  phases were found in different combinations. The clearing temperature decrease from 181 to 170°C with lengthening the terminal alkyloxy-chains from five to twelve carbon atoms. In the second series, recently published by Bedel et al. [8], isophthalaldehyde was used as central part. Depending on the chain length, either  $B_1$  or  $B_2$  phase was observed. For all compounds the transition from a liquid crystalline phase into the isotropic state can be

**TABLE 2** Isomeric series of five-ring bent mesogens



Y	X	X'	Y'
N=CH	COO	OOC	CH=N[7]
COO	N=CH	CH=N	OOC[8]
OOC	N=CH	CH=N	COO <b>2a-2g</b>



observed near to 150°C. These values are comparable to the B<sub>2</sub>-I transition temperatures of the new compounds **2c-2g**, which range from 147 to 153°C, although in this case the sequence B<sub>2</sub>-B<sub>4</sub> occurs. That means that the members of the parent series [7] exhibit the highest mesophase stability. In the other two series the clearing points are decreased and the polymorphism is different.

The structure of the B<sub>4</sub> phase is not yet known. According to X-ray investigations it seems to be a solid phase with a pronounced amount of lattice distortions. The broad diffuse scattering maxima can be explained by a particle-size effect. This is deduced from the fact that the scattering maxima include the main Bragg-reflections of the solid state. The characteristic feature is a transparent blue color [2, 7, 11–14]. According to [12] the blue color is explained by a Rayleigh-like scattering superimposed by self-absorption of the compounds in the near UV region. Sekine et al. [7] proposed a helical superstructure with the helical axis lying parallel to the smectic layers as in twisted grain boundary phases.

Another striking property is the occurrence of domains with opposite optical activity [11–14] which reflect circular polarized light of opposite sign. In addition, the B<sub>4</sub> phase exhibits a SHG signal without an external electric field, which indicates that the molecules are spontaneously non-centrosymmetrically ordered [19–21].

The dielectric measurements done on heating confirm the existence of a relaxation phenomenon in the B<sub>4</sub> phase. The origin of this effect is not cleared up till now, but the existence of the low frequency relaxation points to the fact that the B<sub>4</sub> is not a classical solid phase.

## REFERENCES

- [1] Niori, T., Sekine, T., Watanabe, J., Furukawa, T., & Takazoe, H. (1996). *J. Mater. Chem.*, **6**, 1231.
- [2] Pelzl, G., Diele, S., & Weissflog, W. (1999). *Adv. Mater.*, **11**, 707.
- [3] Shen, D., Diele, S., Pelzl, G., Wirth, I., & Tschierske, C. (1999). *J. Mater. Chem.*, **9**, 661.
- [4] Shen, D., Pegenau, A., Diele, S., Wirth, I., & Tschierske, C. (2000). *J. Am. Chem. Soc.*, **122**, 1593.
- [5] Sadashiva, B. K. (1999). *Pramana*, **53**, 213.
- [6] Thisayukta, J., Nakayama, Y., Kawauchi, S., Takazoe, H., & Watanabe, J. (2000). *J. Am. Chem. Soc.*, **122**, 7441.
- [7] Sekine, T., Niori, T., Sone, M., Watanabe, J., Choi, S. W., Takanishi, Y., & Takazoe, H. (1997). *Jpn. J. Appl. Phys.*, **36**, 6455.
- [8] Bedel, J. P., Rouillon, J. C., Marcerou, J. P., Laguerre, M., Achard, M. F., & Nguyen, H. T. (2000). *Liq. Cryst.*, **27**, 103.
- [9] Weissflog, W., Lischka, C., Diele, S., Pelzl, G., Wirth, I., Grande, S., Kresse, H., Schmalfluss, H., Hartung, H., & Stettler, A. (1999). *Mol. Cryst. Liq. Cryst.*, **333**, 213.
- [10] Weissflog, W., Lischka, C., Benne, I., Scharf, T., Pelzl, G., Diele, S., & Kruth, H. (1998). *Proc. SPIE: Int. Soc. Opt. Eng.* **3319**, 14.

- [11] Sekine, T., Niori, T., Watanabe, J., Furukowa, T., Choi, S. W., & Takezoe, H. (1997). *J. Mater. Chem.*, **7**, 1307.
- [12] Heppke, G., Krüerke, D., Löhning, C., Löttsch, D., Rauch, S., & Sharma, N. K. (1997). *Freiburger Arbeitstagung Flüssige Kristalle*, Freiburg, p. 70.
- [13] Heppke, G., Moro, D. (1998). *Science*, **279**, 1872.
- [14] Collings, P., Heppke, G., Krüerke, D., Löhning, C., Rabe, J., & Stocker, W. (1997). Abstracts of the workshop *Banana-Shaped Liquid Crystals: Chirality by Achiral Molecules*, University of Berlin, Berlin, Germany, p. 15.
- [15] Schmalfuss, H., Weissflog, W., Hauser, A., & Kresse, H. (2000). *SPIE* **4147**, 109.
- [16] Schmalfuss, H., Shen, D., Tschierske, C., & Kresse, H. (1999). *Liq. Cryst.*, **26**, 1767.
- [17] Pelzl, G., Diele, S., Grande, S., Jakli, A., Lischka, Ch., Kresse, H., Schmalfuss, H., Wirth, I., & Weissflog, W. (1999). *Liq. Cryst.*, **26**, 401.
- [18] Salfetnikova, J., Schmalfuss, H., Nádasi, H., Weissflog, W., & Kresse, H. (2000). *Liq. Cryst.*, **27**, 1663.
- [19] Macdonald, R., Kentischer, F., Warnicke, P., & Heppke, G. (1998). *Phys. Rev. Lett.*, **81**, 4408.
- [20] Choi, S.-W., Kinoshita, Y., Park, B., Takazoe, H., Niori, T., & Watanabe, J. (1998). *Jpn. J. Appl. Phys.*, **37**, 3408.
- [21] (a) Kentischer, F., Macdonald, R., Warnick, P., & Heppke, G., *Proc. SPIE: Int. Soc. Opt. Eng.* **3134**, 128 (1998). (b) Kentischer, F., Macdonald, R., Warnick, P., & Heppke, G. (1998). *Liq. Cryst.*, **25**, 341.